

Thermoelectrically Elevated Hydrogel Evaporation for Personal Cooling under Extreme Heat Stress

Yu Pei, Tianshi Feng, Robert Chambers, Shengqiang Cai, Renkun Chen**

Yu Pei, Tianshi Feng, Robert Chambers, Shengqiang Cai, Renkun Chen

Department of Mechanical and Aerospace Engineering, University of California San Diego,
9500 Gilman Drive, La Jolla, CA 92093, USA

Shengqiang Cai, Renkun Chen

Program in Materials Science and Engineering, University of California San Diego, 9500
Gilman Drive, La Jolla, CA 92093, USA

E-mail: s3cai@ucsd.edu; rkchen@ucsd.edu

Keywords: Evaporative cooling, hydrogel, thermoelectrics, extreme heat

Hydrogel evaporative cooling has recently emerged as an appealing strategy for personal cooling. However, with the increasing prevalence of extreme heat events featuring high temperatures (above 40°C) and relative humidity (RH > 30%), hydrogel alone may not achieve thermal comfort under most conditions, as it must be maintained at a sufficiently high temperature—often exceeding the skin comfort temperature (~35.8°C)—to achieve effective evaporation in hot, humid environments. This study integrates thermoelectric devices (TEDs) with hydrogels to create a personal cooling solution suited to extreme heat. TEDs pump heat away from the skin, maintaining it at a comfortable temperature, while simultaneously raising the temperature of a hydrogel layer positioned on top of the TEDs to enhance its evaporation rate. The TED-hydrogel tandem device outperforms TEDs or hydrogel alone in extreme conditions (up to 55°C and RH > 30%). Furthermore, the active temperature control enabled by the TEDs allows the system to adapt to varying thermal loads and environmental conditions. With a manageable hydrogel and battery weight, this cooling system can operate for over six hours. These results demonstrate the potential of hybrid evaporative and thermoelectric cooling as an efficient, adaptable, and sustainable personal cooling solution to combat extreme heat.

1. Introduction

In recent years, extreme heat events have become more frequent due to climate change and the urban heat island effect[1]. The adverse health effects of human heat stress and the health risks associated with prolonged exposure to high temperature have become pressing concerns as global warming continues[2, 3]. Heat-related illnesses account for more than 650 deaths and 65,000 hospitalizations annually in the United States alone, causing more fatalities than all other natural disasters combined [4-6]. These issues are especially severe in regions lacking sufficient nighttime cooling or adequate infrastructure [7]. As a result, there is an urgent need for advanced cooling technologies to mitigate the health risks posed by extreme heat.

Among various cooling strategies, personal wearable cooling devices and garments are gaining attention for their ability to directly cool the skin, providing thermal comfort on the go. This is particularly beneficial for those working outdoors in extreme heat or for individuals without access to air conditioning[8]. Radiative personal cooling device increased the infrared (IR) radiation of human body to passively dissipate heat utilizing materials with high emissivity in the atmospheric transparency window (8-13 μm)[9-12]. While radiative wearable cooling can effectively dissipate heat in certain conditions, its performance is limited in environments with limited view factor to the sky or when the environment is too hot. Evaporative cooling, where liquid transforms into vapor by absorbing heat due to its high latent heat, is a powerful method of thermal regulation that we encounter frequently in daily life [13]. The evaporation of sweat plays a key role in the body natural heat dissipation of the body in hot environments[14-16]. Consequently, there has been extensive research into easy-to-use evaporative cooling systems for personal thermal regulation. Moisture-responsive textiles that enhance vapor permeability when activated have shown notable cooling performance compared to standard fabrics[17-19]. However, these textiles depend on sweat evaporation from the skin and are therefore less effective in extreme heat exceeding 40°C, as sweating at such high temperatures can lead to discomfort.

Alternatively, evaporative cooling can be achieved through textiles that contain water. In particular, hydrogel—a material composed of gel networks with a high water content—offers a promising approach, as it can be easily applied as a coating on textiles to induce evaporative cooling from the stored water. This enhanced thermal management capability has been demonstrated in various electronic systems[20, 21] and holds potential for personal thermal

management applications. For instance, Fei et al. developed a hydrogel-based composite capable of providing sub-ambient cooling power of 350 W m^{-2} in environments up to 36°C [22]. Later, Hu et al. demonstrated a continuous cooling effect lasting up to an hour under metabolic heating in ambient temperatures averaging 43°C , using a hierarchically porous hydrogel composite[23]. Li et al. report a method for spary-coating porous hydrogel coatings over large areas which can enhance hydrogel cooling efficiency[24]. However, the operational temperature limit remains below 45°C , insufficient to counter extreme temperatures above 50°C observed in many regions around the globe[25-27].

One limitation is the low surface temperature of the hydrogel, which affects the evaporation rate. When the skin temperature is maintained at a comfortable level around 35°C , the evaporation surface temperature of the hydrogel is determined by its thermal resistance and metabolic heat generation rate. Typically, with a 5 mm thick hydrogel, a temperature drop of about 2°C across the hydrogel layer is required (Figure 1d), resulting in a surface temperature of around 33°C . This temperature is insufficient to drive rapid evaporation in the hot and humid conditions of extreme heat, thereby reducing the effectiveness of hydrogel in such environments.

To address the limitations of current hydrogel-based personal cooling devices in extreme heat, we propose a hybrid wearable cooling garment that combines hydrogel with thermoelectric devices (TEDs), as shown in Figure 1a. TEDs have been extensively explored as personal cooling solutions due to their lightweight, solid-state structure, and active controllability[28-31]. Previous research has primarily focused on developing wearable TEDs for small, limited functional areas (typically less than $5 \times 5 \text{ cm}^2$)[32-35]. A few studies have explored larger cooling areas using TED-water circulation hybrid systems[36, 37]; however, these designs often require bulky heat sinks and are limited by operating temperature constraints, reducing their effectiveness under extreme heat conditions.

Building on our previous work[38] in optimizing thermal design to establish an ideal temperature gradient across TEDs, we combine TEDs and hydrogel to effectively elevate the surface evaporation temperature of the hydrogel on the TEDs' hot side, while maintaining a comfortable temperature on the cold side. This TED-hydrogel composite is integrated into a fabric, creating a wearable active cooling garment designed to perform under extreme heat conditions (Figure 1). During operation, the hydrogel absorbs heat from the hot side of the TED, initiating sufficient evaporation to dissipate both metabolic heat and excess TED-generated heat. As shown in Figure 1d, the TED-hydrogel device achieves a higher surface

temperature in the hydrogel, resulting in a more efficient evaporative cooling rate than hydrogel alone. Consequently, this TED-hydrogel integration enables more effective cooling of the skin in the same ambient conditions.

We evaluated the impact of hydrogel surface temperatures on evaporation rates through evaporation rate testing. Our findings show the importance of high surface temperatures for achieving optimal evaporation. COMSOL simulations further validated that the TED-hydrogel composite significantly exceeds the cooling rates achievable by hydrogel alone. Testing in controlled environments, with ambient temperatures from 40°C to 55°C and relative humidity levels of 30%-50%, demonstrated that the device consistently maintained skin temperatures within the comfort threshold of 35.8°C[13] across all tested conditions, even at an ambient temperature of 55°C. The adaptability of the system was further highlighted by its response to varying thermal loads typical of different activities, ranging from 50 to 150 W m⁻². Long-term durability tests showed that garment with 5 mm thick hydrogels effectively operated for over six hours. Integrating a temperature controller with the TED-hydrogel device ensured stable skin temperatures when subjected fluctuating environmental conditions, showcasing the benefits of dynamic temperature regulation over traditional passive cooling methods.

Our study demonstrates that the TED-hydrogel integration offers a novel approach to personal cooling, meeting the demand for more effective and adaptable personal cooling solutions amid global temperature rises. With a sustained performance over several hours, this system is well-suited for outdoor workers and those vulnerable to heat-related illnesses in increasingly hot climates.

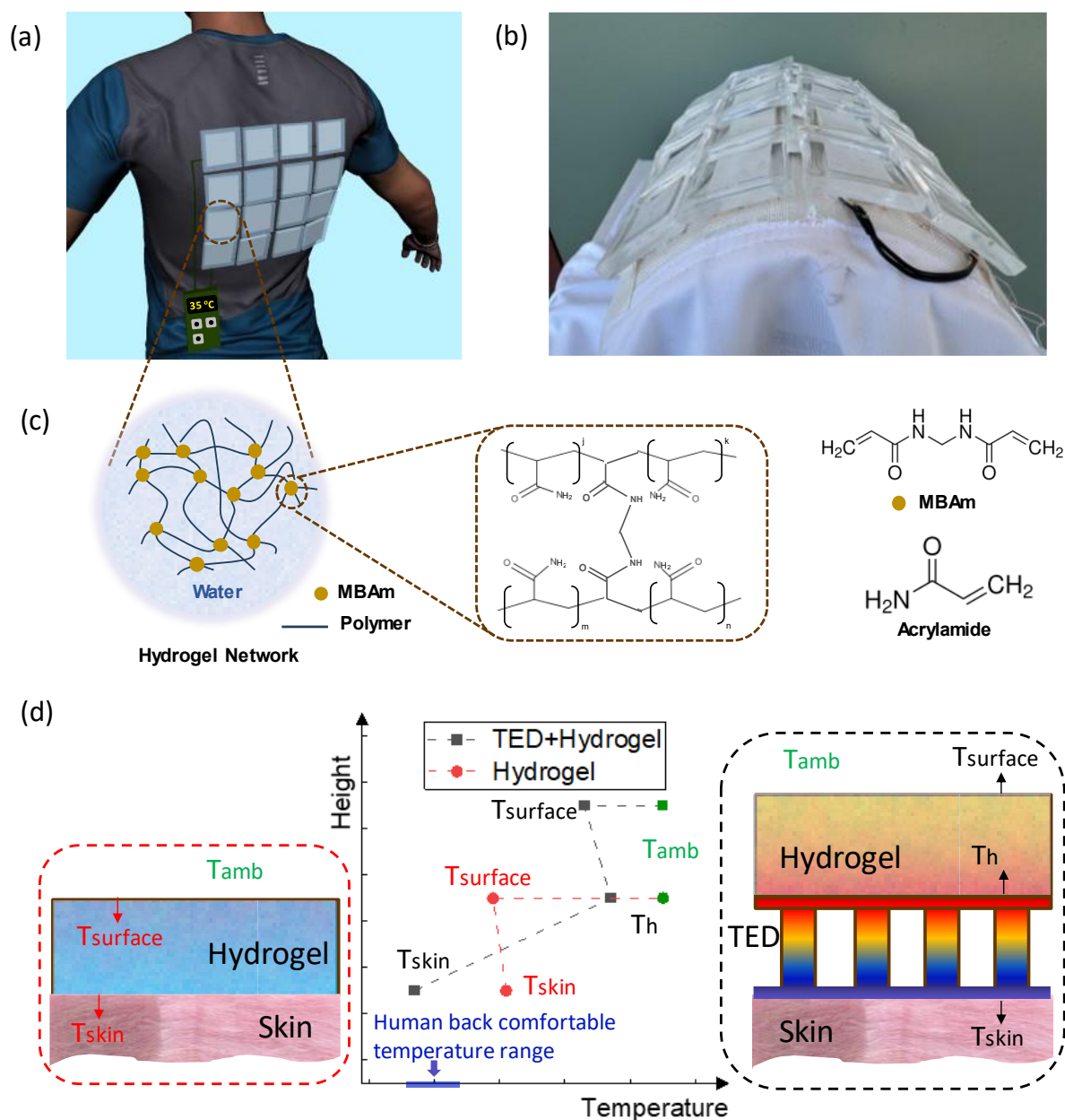


Figure 1. Novel personal cooling garment integrating thermoelectric devices and hydrogel (TED-hydrogel). a) Schematic of the TED-hydrogel personal cooling garment. b) Photograph of the flexible, wearable TED-hydrogel active cooling garment. c) Schematic and chemical formula of the polyacrylamide (PAAm) hydrogel, with methylenebisacrylamide (MBAm) as a cross-linker for acrylamide (AAm) monomers, forming a hydrogel network through polymerization. d) Temperature distribution along the thickness direction for the hydrogel and TED-hydrogel device. T_{skin} represents the interface temperature between the hydrogel and the skin, or between the cooled TED side and the skin. T_{h} denotes the hot side temperature of the TED, T_{surface} is the top surface temperature of hydrogel, and T_{amb} is the ambient temperature.

The shaded blue bar on the x-axis represents the comfortable temperature range for the human back.

2. Results

2.1. Hydrogel Evaporation rate

The evaporation rate of the hydrogel is closely linked to the ambient environment and its surface temperature. To investigate this, we conducted a mass loss test. Figure 2a shows the experimental setup, where a 4 cm × 4 cm × 5 mm hydrogel sample was placed on a balance in an environmental chamber with controlled temperature and humidity. After thermal equilibrium, the hydrogel surface temperature was measured using an IR camera (Figure 2b). Due to evaporative cooling, the hydrogel surface temperature was lower than the ambient temperature (T_{amb}), with the difference depending on both environmental temperature and humidity. For example, Figure 2b shows that the hydrogel surface temperature is about 33 °C when the ambient temperature is 40 °C and the relative humidity is ~45% ($T_{amb} = 40^{\circ}\text{C}$, RH ~45%). At the same ambient temperature, lower RH led to a lower hydrogel surface temperature due to a higher evaporation rate. We calculated the mass loss ratio, $\frac{m_0 - m(t)}{m_0}$, by recording the initial weight m_0 and real-time weight $m(t)$ over time. Mass loss was measured at two ambient temperatures (40°C and 50°C) and two humidity levels (30–35% RH and 45–50% RH).

Evaporation from a surface is affected by ambient temperature (T_{amb}), air humidity, surface water temperature (T_s), and air velocity above the water surface (v). Here, we assume that the evaporation of hydrogels is the same as the evaporation of free water. The evaporation rate g_s [$\text{kg s}^{-1} \text{m}^{-2}$] can be described by the equation[20]:

$$g_s = (25 + 19v) * (X_s - X_{sair}) * 3600 \quad (1)$$

where X_s is the maximum humidity ratio of saturated air at the surface temperature, X_{sair} is the the humidity ratio of air at ambient temperature.

Further evaporation calculations are detailed in Supporting Information Note 1. Calculation results for the mass loss ratio, represented by the shaded areas in Figure 2c, show good agreement with experimental data. The upper and lower limits of the shaded area were obtained

by considering the hydrogel surface temperature range in the evaporation rate equation. At a given ambient temperature, lower humidity results in lower hydrogel surface temperatures and a higher evaporation rate, while at a fixed RH, higher ambient temperatures leads to higher hydrogel surface temperatures and higher evaporation rates.

Figure 2d shows the calculated evaporation rate as a function of ambient and hydrogel surface temperatures, with the right z-axis converting the evaporation rate into the corresponding heat flux from hydrogel evaporation. Experimental results in Figure 2c show that the difference between ambient and hydrogel surface temperatures ($T_{amb} - T_s$) increases as T_{amb} rises. Calculation results in Figure 2d indicate that when this difference is large, the evaporative cooling power of hydrogel is minimal. Additionally, when T_{amb} is significantly higher than T_s , convection and radiation heat flux from the environment to the hydrogel becomes important, which may result in heating, rather than cooling, of the skin.

To evaluate the suitable conditions for hydrogel evaporative cooling, we used COMSOL simulations to estimate the cooling power of hydrogel under various temperature and humidity conditions (details in the experimental section). The bottom temperature of hydrogel (representing target skin temperature) was set to 34°C. The calculated net cooling power provided by the hydrogel under different conditions is shown in Figure 2e. For temperatures below 40°C, the hydrogel dissipated heat fluxes of 50–150 W m⁻² effectively. However, at ambient temperatures above 40°C and RH levels above 30%, the evaporation rate is limited by the hydrogel temperature. In these conditions, hydrogel evaporation cannot provide sufficient cooling to offset metabolic heat. In fact, when ambient temperatures above 42°C and RH levels above 30%, the net cooling power becomes negative, indicating that radiation and convection heat flux from the hotter environment overwhelms the evaporation cooling flux.

To overcome the limitation of inadequate evaporation when the hydrogel temperature is below ambient temperature, especially at higher humidity levels, we propose a TED-hydrogel tandem device consisting of a hydrogel layer placed on top of the hot side of the TED while the cold side of the TED is in contact with the skin. As shown in Figure 1d, the TEDs not only add cooling capacity to the skin but also elevates the hydrogel temperature to achieve high evaporation rate. The TED design was selected based on our previous work [31], which was optimized to establish a large temperature difference between the hot and cold sides and is thus suitable for the purpose of elevating the hydrogel temperature. We developed a COMSOL model to evaluate the system performance, considering hydrogel evaporation, thermoelectric

effects, and heat transfer between the device and the environment. As shown in Figure 2e, simulations of the TED-hydrogel hybrid demonstrate significant improvements in cooling capacity, even at ambient temperatures up to 55°C and 50% RH. In the simulated temperature distribution (Figure 2f), while the bottom surface of the TED-hydrogel tandem remains at 34°C, the top surface of the hydrogel reaches up to 50°C due to the heat pumping of the TEDs, significantly enhancing the evaporation rate of water in hydrogel.

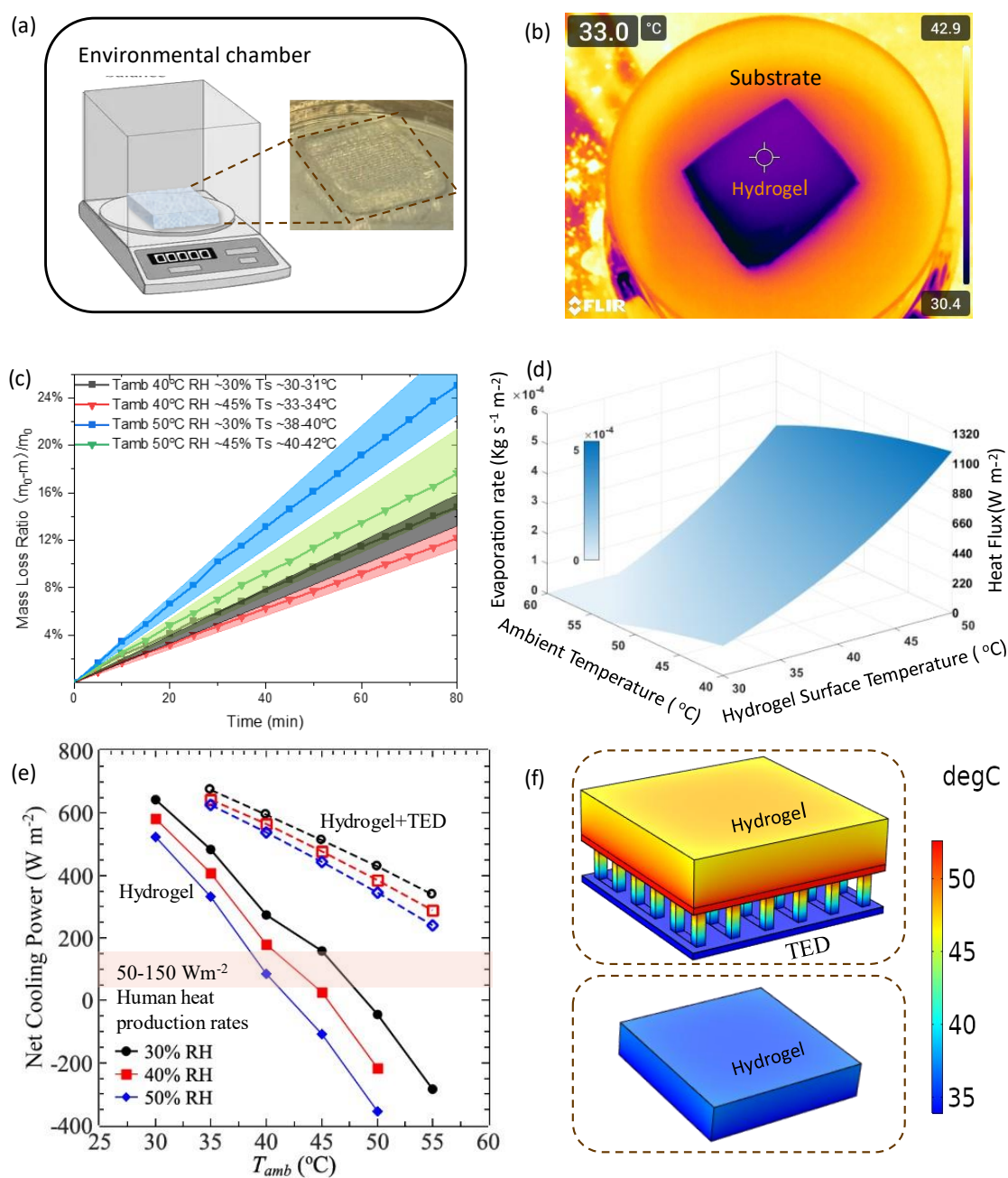


Figure 2. Hydrogel evaporation rate and cooling power. a) Setup for measuring hydrogel mass loss. b) Infrared (IR) image showing the hydrogel surface temperature (T_s) during evaporation (ambient temperature $T_{amb} = 40^\circ\text{C}$ and relative humidity $\text{RH} \sim 45\%$). The purple region

represents the hydrogel, which has a lower temperature than the ambient due to evaporative heat dissipation. c) Measured (lines and symbols) and calculated (shaded areas) hydrogel mass loss ratio. The mass loss ratio is defined as the mass loss $m_0 - m(t)$ divided by the original hydrogel weight m_0 . Calculations used the range of hydrogel surface temperatures (T_s), as shown in the legend. d) Calculated hydrogel evaporation rate under different ambient temperatures (with RH fixed at 30%) and hydrogel surface temperatures. The right z-axis represents the corresponding heat flux from water evaporation, which is the mass of evaporated water multiplied by latent heat. e) COMSOL simulation results showing net cooling power as a function of ambient temperature for hydrogel alone (symbols + solid lines) and hydrogel + TED (symbols + dashed lines). The shaded band represents the metabolic rate. Net cooling power includes evaporative cooling minus the heat transfer rate from ambient to skin, with skin temperature fixed at 34°C. f) Temperature distribution for hydrogel alone and TED-hydrogel from the COMSOL model at $T_{\text{amb}} = 55^\circ\text{C}$, RH = 30%, and net cooling power of 338 W m^{-2} for the TED-hydrogel device and -284 W m^{-2} for hydrogel alone. The negative net cooling power of the hydrogel-only case means the heat gain from the hot environment outweighs the evaporative cooling from the hydrogel.

2.2. Single TED-hydrogel cooling device

To experimentally test our concept, we first used a single TED ($2.3 \times 2.3 \text{ cm}$) in combination with a $2.5 \text{ cm} \times 2.5 \text{ cm} \times 5 \text{ mm}$ hydrogel sample. A heater was placed beneath the TED to simulate the metabolic heat flux from human skin. When current was applied, the bottom surface of the TED cooled while the top surface heated, with the combined heat from the TED and the heater being dissipated through hydrogel evaporation. This setup was placed in an environmental chamber with controlled temperature and humidity. Figure 3a shows a schematic of the experimental setup, where the heater was connected to a power supply, and the temperatures on the hot and cold sides of the TED were measured using thermocouples connected to a data acquisition (DAQ) module (HP HEWLETT PACKARD 34970A) for data recording. The TED was connected to a voltage source (Agilent E3634A) controlled by a computer to adjust the applied voltage. Figure 3b shows an image of the experimental TED-hydrogel device.

Figures 3c and 3d present the experimental results under different ambient temperatures (40°C , 45°C , 50°C , and 55°C) and relative humidity levels (30–35% RH and 45–50% RH),

with heat flux of 100 W m^{-2} on the heater. The voltage applied to the TED ranged from 0.1 to 1V. As the voltage increased, the cold side temperature (T_c) of the TED—representing skin temperature—decreased, while the hot side temperature (T_h) increased. Both T_c and T_h rose as the ambient temperature increased. Comparing Figures 3c and 3d, we can also conclude that higher humidity levels led to higher T_c and T_h at the same ambient temperature, as the hydrogel evaporation rate decreases at higher humidity. Figures 3e, 3f, and 3g display the results of long-term stability tests on the TED-hydrogel cooling device at a constant applied voltage of 0.6V under varying temperature and humidity conditions. In all scenarios, the TED-hydrogel tandem device maintained the skin surface temperature below 31°C , with stable performance for over an hour.

For comparison, we also conducted an experiment with hydrogel placed directly on the heater (i.e., hydrogel only, inset of Figure 3f). The results from Figures 3e, 3f, and 3g show that the hydrogel only case has about 5°C higher cold side temperature compared to that of TED-hydrogel under all testing conditions. In particular, at ambient temperature of 45°C and RH of 45-50 % (Figure 3f) or ambient temperature of 50°C and RH of 30-35 % (Figure 3g), the hydrogel only case had cold side temperature of about 37°C , above the skin thermal comfort range. This result again demonstrates that the TED-hydrogel device can provide adequate cooling for human skin under extreme conditions where hydrogel alone cannot.

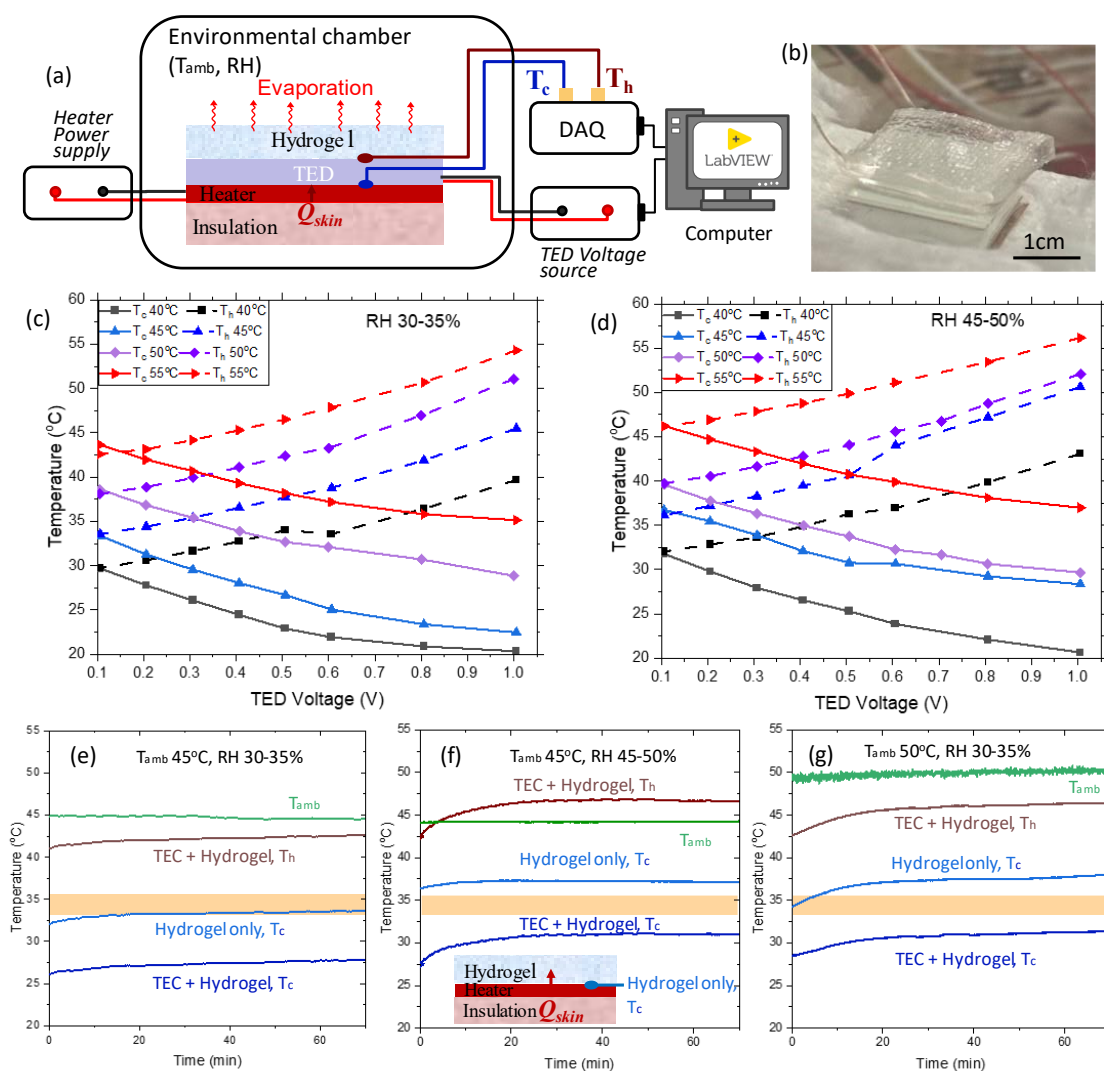


Figure 3. Performance of a single TED-hydrogel cooling device. a) Measurement setup for the TED-hydrogel device. The power supply delivers a heat flux of 100 W m^{-2} to the heater to simulate human metabolic heat flux. The computer controls the TED voltage supply and records the temperatures of the cold (T_c) and hot (T_h) sides of the the TED. b) Photograph of the single TED-hydrogel cooling device. Temperature results for the cold and hot sides of the TED-hydrogel device under different ambient temperatures and humidity conditions: c) RH 30–35% and d) RH 45–50%. Solid lines represent T_c and dashed lines represent T_h at various TED voltages. Long-term tests for the single TED-hydrogel device and hydrogel alone at a constant applied voltage of 0.6V under varying temperature and humidity conditions: e) $T_{\text{amb}} = 45^\circ\text{C}$, RH 30-35%. f) $T_{\text{amb}} = 45^\circ\text{C}$, RH 45-50%. g) $T_{\text{amb}} = 50^\circ\text{C}$, RH 30-35%. The shaded yellow area represents the comfortable temperature range for the human back ($33.8\text{--}35.8^\circ\text{C}$) [13]. The inset

in f) shows the schematic setup for testing hydrogel alone, with T_c (of hydrogel only) indicating the temperature at the hydrogel bottom surface in contact with the heater.

2.3. TED-hydrogel Personal Cooling Garment

After confirming the feasibility of the TED-hydrogel device for personal cooling, we designed a personal cooling garment, shown in Figure 4a. The garment consists of a 4×4 array of TEDs attached to a fabric with high thermal conductivity, with each TED covered by a hydrogel layer on the top to dissipate heat. The spacing between TEDs allows the garment to remain flexible and comfortably conform to the curvature of the human back. Figure 4b illustrates the cross-section of the cooling setup.

In addition to measuring the hot side temperature (T_h) and cold side temperature (T_c) of the TEDs, we monitored the fabric temperature at the center of the TED array (T_m), representing the highest temperature on the fabric. The garment was tested in an environmental chamber under different temperatures (45°C and 50°C) and humidity conditions (30–35% RH and 45–50% RH). The TED array was wired into two parallel strings, each with eight TEDs in series. The total applied voltage ranged from 1–9V. As shown in Figures 4b and 4c, the garment effectively maintained temperatures below 35°C in low-humidity conditions (30–35% RH) at both 45°C and 50°C ambient temperatures. In higher humidity (45–50% RH), cooling performance decreased due to a lower evaporation rate, though T_c remained within the thermal comfort range at both temperatures.

To simulate various human activities with different metabolic heat rates (e.g., resting or sitting at $\sim 45\text{--}55 \text{ W m}^{-2}$, slow walking at $\sim 110 \text{ W m}^{-2}$, and fast walking at $\sim 140 \text{ W m}^{-2}$)[39], we conducted additional tests with varying heater power levels. As shown in Figure 4d, the TED-hydrogel cooling garment performed effectively at 50°C ambient temperature and 30–35% RH across a range of simulated body heat flux levels up to 150 W m^{-2} .

We also conducted long-term tests with hydrogels of different thicknesses (5 mm and 3 mm). The 5 mm hydrogel maintained T_c below 35.8°C for over 6 hours, while the 3 mm hydrogel lasted for 4 hours. As shown in Figure 4e, T_c initially dropped to as low as $\sim 28^\circ\text{C}$, and T_h increased sharply within minutes due to the heat pumping of the TED to its hot side, after which temperatures remained stable for approximately 100 minutes. Subsequently, all temperatures gradually rose as the hydrogel was losing water, causing it to shrink laterally and reducing cooling power due to decreased evaporating surface area. Eventually, the hydrogel surface area

became smaller than the TED, causing the edges of the hydrogel to peel off and resulting in a rapid rise in both T_c and T_h . Throughout the test, the temperature at the center of the fabric (T_m) remained a few degrees higher than T_c due to the lateral thermal resistance of the fabric.

The initial weight of the 16 pieces of 5 mm hydrogel was 154.46 g, which decreased to 58.55 g after 7 hours, reflecting a 61% mass loss. The average evaporation rate, calculated as $\frac{m_0 - m}{t * A}$, where A is the area and t is time, was $1.6853 \times 10^{-4} \text{ kg s}^{-1} \text{ m}^{-2}$, matching the calculated value of $1.835 \times 10^{-4} \text{ kg s}^{-1} \text{ m}^{-2}$ (Figure 2d). For the 3 mm hydrogel, the mass loss was 66% (from 93.78 g to 31.56 g) after 4.5 hours, with an average evaporation rate of $1.753 \times 10^{-4} \text{ kg s}^{-1} \text{ m}^{-2}$. We note that the hydrogel can be restored to its original size by soaking in water for 1–2 hours.

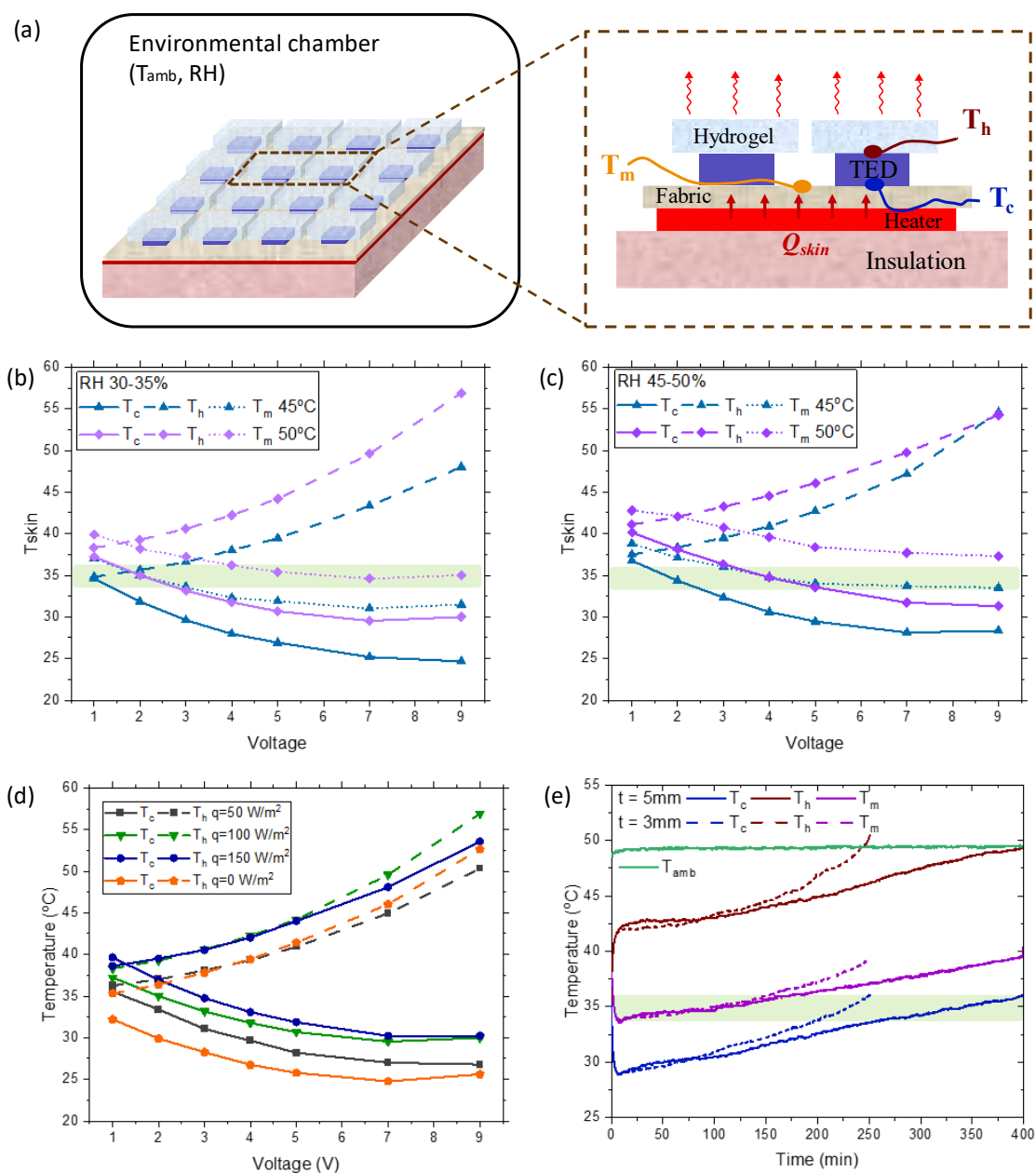


Figure 4. Performance of the TED-hydrogel personal cooling garment. a) Schematic diagram of the 4×4 TED-hydrogel personal cooling garment test setup. Measured values of T_c , T_h , and T_m (the temperature at the center of the fabric) under different TED voltage levels and ambient temperatures in b) 30–35% RH and c) 45–50% RH environments. The heater heat flux (q) is set to 100 W m^{-2} . d) T_c (symbols + solid lines) and T_h (symbols + dashed lines) at 50°C ambient temperature and 30–35% RH, under varying human body heat flux levels. The voltage applied to the entire TED array in the garment ranged from 1 to 9V. e) Long-term test results for hydrogels with different thicknesses (dashed line for 3 mm and solid line for 5 mm) at 50°C ambient temperature, 30–35% RH, and $q = 100\text{ W m}^{-2}$. The voltage applied to TEDs is 5V. The

shaded green area represents the comfortable temperature range for the human back (33.8–35.8°C).

By assembling the TED-hydrogel cooling device with a PID (Proportional-Integral-Derivative) temperature controller and a battery pack, we tested the personal cooling garment in a real-world environment with varying temperature and humidity (Figure 5a). The DC output from the battery pack was connected to the temperature controller as the power input, and the controller output supplied the power to the TEC array. The controller generates a fixed-period square wave with preset maximum and minimum voltage values, adjusting the duty cycle based on the temperature setpoints.

Figures 5c and 5d show the resulting T_c , T_h , and T_m values with ambient temperature of 45°C in different humidity environments, with similar results at 40°C presented in Supplementary Figure S1. The red line indicates the average output current from the battery pack. As shown, T_c closely followed the temperature setpoint, while T_m remained a few degrees higher but followed the same trend. T_h increased as the set temperature decreased. At 45°C ambient temperature and 45–50% RH, T_c began to deviate from the setpoint around 30°C as the battery pack reached its maximum output capacity.

Figure 5b shows IR images of the TED-hydrogel front (hot) and back (cold) sides of the cooling device when operating at an ambient temperature of 45°C and 45–50% RH. The back side maintained a temperature close to the setpoint (34°C), within the comfortable range for the human back. The top surface of the hydrogel reached a significantly higher temperature than the cold side of the TEDs, enabling an elevated evaporation rate for effective heat dissipation.

Recognizing that ambient temperatures in real-world applications may fluctuate, we conducted tests with dynamic ambient temperatures (ranging from 40–45°C) at 45–50% RH. Figure 5e shows the results of this dynamic test, with the temperature setpoint fixed at 34°C and the heater providing a heat flux of 100 W m⁻². Despite changes in ambient temperature from 40°C to 45°C, T_c remained stable at the set temperature, while T_m remained stable and 2–3°C higher than T_c . The hot side temperature of the TEDs increased as T_{amb} rose. The gray shaded area represents the power output from the temperature controller to the TED array, which increased as the ambient temperature rose.

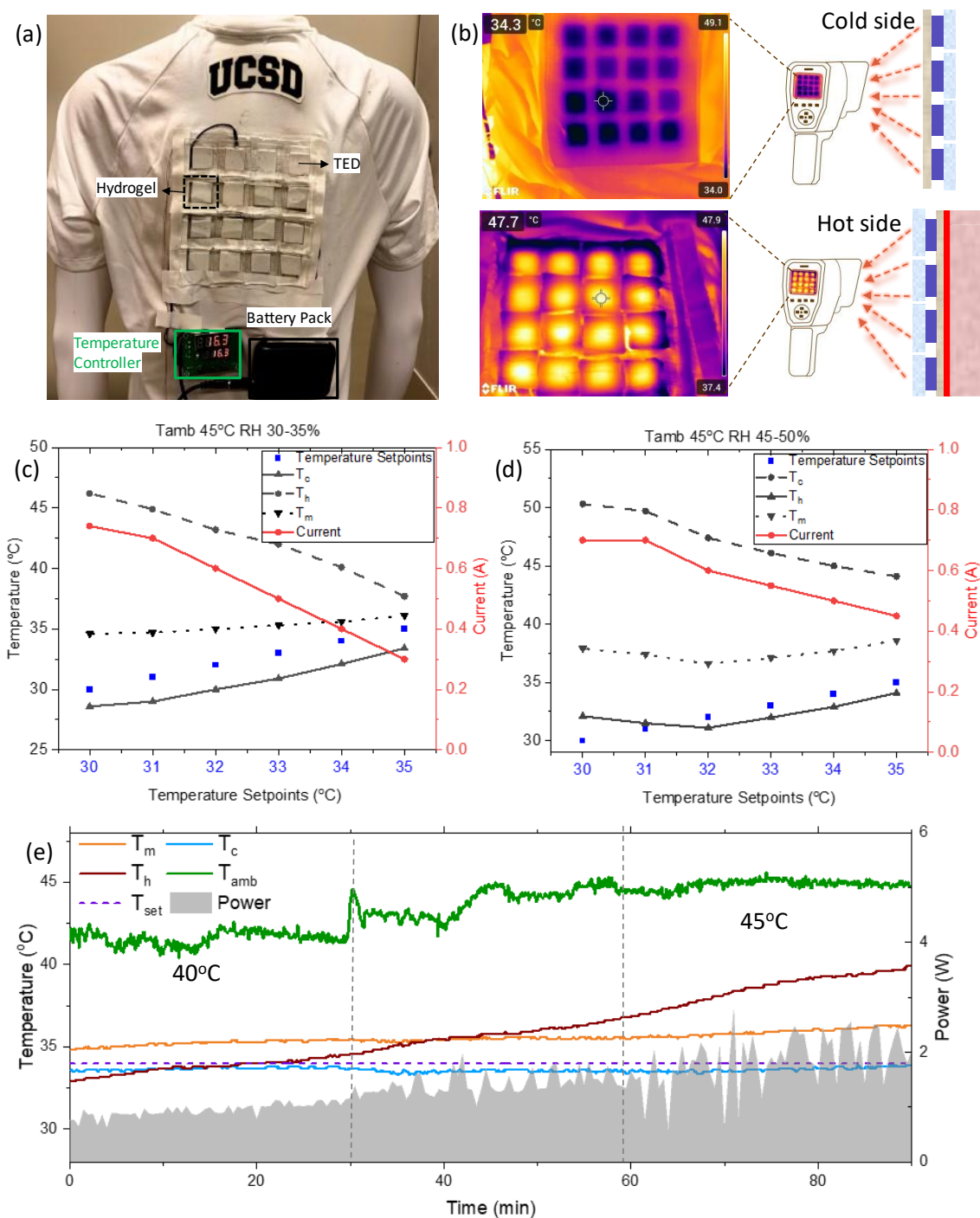


Figure 5. Temperature-controlled wearable TED-hydrogel device. a) Photograph of the TED-hydrogel personal cooling garment equipped with a temperature controller and a battery pack. b) IR images of the cold side (taken from the fabric attached to the cold side of the TED) and the hydrogel side (taken from the top surface of the hydrogel) of the TED-hydrogel device, with ambient temperature at 45°C and RH at 30–35%. TED-hydrogel device response under different set temperatures at 45°C in c) 30–35% RH and d) 45–50% RH. The blue dots represent the set temperature by the controller. Solid, dashed, and dotted lines represent T_c , T_h , and T_m ,

respectively. The red dots correspond to the y-axis on the right, indicating the average current input to the TED array by the controller. e) Test results for the TED-hydrogel device under dynamic ambient temperatures (from 40°C to 45°C). The gray shaded area corresponds to the y-axis on the right, representing the power input to the TED. All tests in this figure used a 100 W m⁻² heat flux for the heater.

3. Discussion

We summarize the cooling performance of the TED only, hydrogel alone, and the TED-hydrogel combination in Figure 6. The data for the TED only case is from our recent work [40], where a fan was used as a heat sink. All three methods demonstrate notable cooling power compared to the baseline without any cooling device. At an ambient temperature of 40°C, the temperature differences achieved are 12.33°C for the TED with a fan, 15.9°C for hydrogel alone, and 26.9°C for the TED-hydrogel combination. The TED with a fan provides effective cooling at ambient temperatures below 40°C. However, at temperatures above 40°C, convective heat dissipation alone cannot adequately remove the heat generated by the hot side of the TED. In contrast, hydrogel alone shows better cooling performance than the TED with a fan at higher temperatures, though its cooling capacity becomes insufficient in environments above 45°C. Among the three methods, the TED-hydrogel device shows the best cooling performance. The TED contributes substantial cooling power, while the hydrogel serves as an effective heat sink. As the TED heats the hydrogel, the elevated temperature increases the evaporation rate, enhancing heat dissipation. This synergy between the TED and hydrogel accounts for the superior performance of the TED-hydrogel combination shown in Figure 6.

Hydrogel is a promising material for passive personal cooling due to its ability to dissipate heat through evaporation. However, its cooling power alone is limited by the relatively low evaporation rate under typical ambient conditions. Achieving a higher evaporation rate would require a consistently high hydrogel surface temperature, which would be too high for the skin. TED is a widely used cooling technology, but its effectiveness depends heavily on efficient heat dissipation from the hot side, typically achieved with a solid heat sink or fan. Our research demonstrates that hydrogel is a more effective heat dissipation medium for TEDs than conventional methods. The TED-hydrogel combination leverages the benefits of both systems: the TED provides active cooling and raises the temperature of hydrogel, while the hydrogel enhances heat dissipation through evaporation at elevated temperature.

Additionally, the TED-hydrogel device offers better control over skin temperature by adjusting the TEDpower output in response to environmental changes. In contrast, hydrogel alone varies in effectiveness with environmental conditions, potentially leading to skin temperatures that are either too high or too low for thermal comfort. This makes the TED-hydrogel combination a more reliable and adaptable solution for personal cooling across diverse environmental conditions.

For real-world application, the weight of the garment is important. The total weight of the garment studied here is approximately 530 g: ~154 g for 16 pieces of 5 mm thick hydrogel: 256 g for the battery pack power bank, 88 g for the 16 TEDs, and ~31 g for the temperature controller. There is a correlation between the system weight and the cooling duration, primarily due to the capacity of the battery pack and the hydrogel. The battery pack shown here has a capacity of 59.2 Wh (16,000 mAh/3.7V). Based on the maximum power consumption of 5.5 W at 50 °C ambient temperature, the battery can operate the garment for about 12 hours, more than sufficient to sustain the cooling duration of the 5 mm thick hydrogel (~ 6 hours). If a lighter garment is desirable, one could opt to use a smaller battery pack and thinner hydrogel. For example, for the 3 mm hydrogel, the original weight was 93.78 g while the cooling duration was also shortened to about 4.5 hours. If a smaller battery pack with one third of the capacity and cooling duration was used (~20 Wh, for ~ 4 hr duration, and weight of ~ 85 g), the total garment weight would be about 300 g.

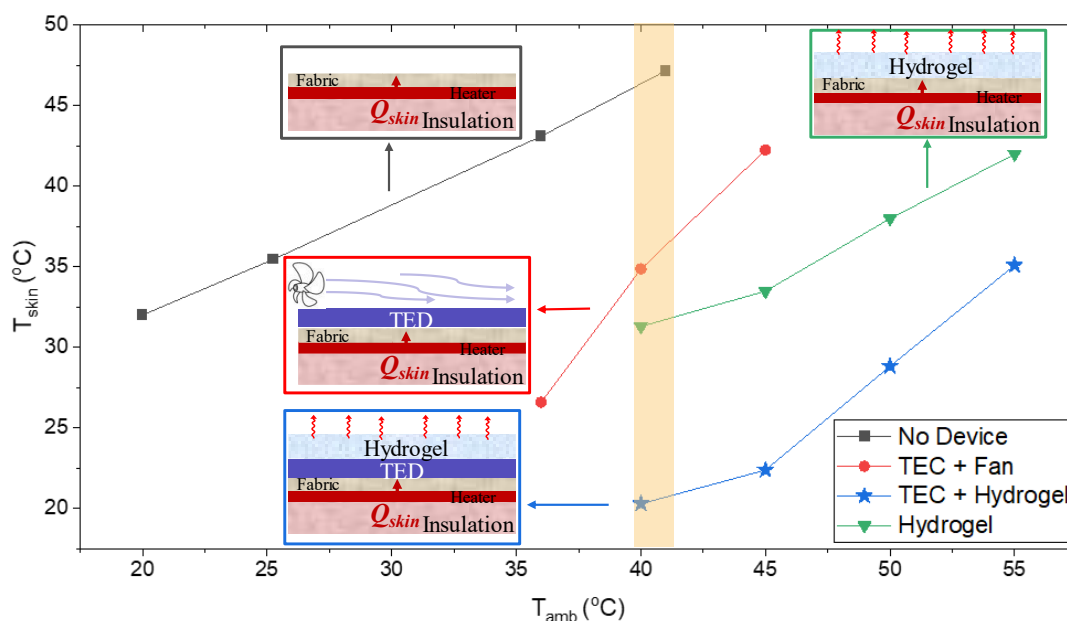


Figure 6. Cooling performance of the TED with a fan (red circle), hydrogel alone (green triangle), and the TED-hydrogel combination (blue star). The black line and curve square dots represents the fabric temperature variation with ambient temperature without any cooling device. The data for TED with a fan and without any cooling device is from our previous work[40]. The shaded yellow area highlights the ambient temperature range around 40°C. The relative humidity for all tests was maintained at approximately 30–35%.

4. Conclusion

In conclusion, this study demonstrates that integrating thermoelectric devices (TEDs) with hydrogels provides a powerful and adaptable personal cooling solution that outperforms each component alone, particularly under extreme environmental conditions (up to 55°C and RH > 30%). By actively raising the hydrogel surface temperature, TEDs enhance the evaporative cooling effect of hydrogel, delivering stable cooling in both constant and fluctuating temperatures and humidity levels representative of extreme heat. Experimental results show that the TED-hydrogel combination can maintain a skin-like surface temperature below the thermal comfort threshold of 35.8°C for extended periods (over 6 hours with a 5 mm hydrogel layer), significantly increasing the evaporation rate and heat dissipation. In real-world applications, the flexible TED-hydrogel personal cooling garment not only improves cooling efficacy but also enhances adaptability, supporting sustainable thermal comfort in extreme heat.

This research paves the way for the advancement of personal cooling technologies to combat extreme heat conditions that are increasingly intensified by climate change.

5. Experimental Section

COMSOL Model of Hydrogel Evaporation: The thermal performance of hydrogel evaporation was simulated using the COMSOL Multiphysics Heat Transfer Module, with hydrogel thermal properties assumed to be the same as water. The bottom surface of the hydrogel was set at a constant temperature of 34°C. Convection, radiation, and evaporation boundary conditions were applied to the top and side surfaces, with the hydrogel emissivity assumed to be 0.9 under natural convection. The evaporation rate was determined by Equation (1), which estimates pure hydrogel evaporation as a function of hydrogel surface temperature, ambient temperature, and relative humidity. A stationary study was conducted to simulate the experimental steady state, and the cooling power was extracted as the total normal heat flux at the bottom surface.

COMSOL Model of the Hybrid System (TED+Hydrogel): The TED performance was simulated by combining the thermoelectric effect and electromagnetic heating modules in COMSOL. The model geometry was constructed based on the device size and its 36 thermoelectric (TE) pillars, as well as the air layer between two alumina substrates. A constant temperature boundary condition of 34°C was applied beneath the bottom alumina substrate. The top of the alumina substrates was covered with a hydrogel layer, serving as an additional heat sink. Radiation and convection boundary conditions were applied to all surrounding and top surfaces, with the same evaporation rate boundary condition as in the hydrogel-only model. Using a stationary study with an input current of 250 mA, the cooling power was calculated by extracting the total heat flux at the bottom TED surface.

Materials: All chemicals were used as received without further purification. Acrylamide (AAm; Sigma-Aldrich 01700), N,N'-methylenebis(acrylamide) (MBAm; Sigma-Aldrich M7279), Ammonium persulfate (APS; Sigma-Aldrich A3678), and N,N,N',N'-tetramethylethylenediamine (TEMED; Sigma-Aldrich T9281) were used in hydrogel synthesis.

Synthesis of PAAm Hydrogel: Polyacrylamide-based hydrogel synthesis involved the polymerization of acrylamide (AAm) monomers, cross-linked by N,N'-methylenebis(acrylamide) (MBAm). Ammonium persulfate (APS) served as the initiator,

generating free radicals to start polymerization, while tetramethylethylenediamine (TEMED) acted as a catalyst to accelerate polymerization by promoting radical formation from APS. After combining all components, the polymerization formed a flexible, hydrophilic three-dimensional hydrogel network. Hydrogel synthesis methods were adapted from previous work[32].

Three solutions and TEMED were mixed to form the polymer precursor, which was then poured into the mold. Solutions were separately prepared and stirred with a magnetic stirrer until homogenous. Solution (1) was prepared with 25 wt% monomer, combining 30 g AAm and 90 g deionized water. Solution (2) consisted of 10 g deionized water and 0.2 g MBAm (2 wt%). Solution (3) contained 10 g deionized water and 0.5705 g APS (0.25 M). The mixing ratio was 1 g of solution (1), 9 μ L of solution (2), 8 μ L of solution (3), and 0.8 μ L TEMED. For a batch using 120 g of solution (1), 1080 μ L of solution (2), 960 μ L of solution (3), and 96 μ L of TEMED were added to solution (1) while stirring.

The mold consisted of a 4×4 cavity array. A laser-cut acrylic sheet was adhered to a glass plate using VHB to create a watertight mold. The upper glass plate, cavities, and lower glass plate were treated with RainX to facilitate release. After preparing the precursor solution, a transfer pipette was used to fill the mold, slightly overfilling each cavity. The upper glass plate was then lowered carefully and secured with weights. The mold was held at room temperature for 1 hour to partially cure the hydrogel, followed by 2 hours in a 45°C oven. Once cured, the hydrogel was demolded.

Supporting Information

Supporting Information is available from the Wiley Online Library or from the author.

Acknowledgements

This work is supported by California Climate Action Seed Awards 2023 Program (Award ID: R02CP7256, for hydrogel synthesis and characterization) and National Science Foundation (CMMI-1762560, for thermal measurements).

References

- [1] L. Keith, S. Meerow, and T. Wagner, "Planning for extreme heat: a review," *Journal of Extreme Events*, vol. 6, no. 03n04, pp. 2050003, 2019.

- [2] O. Jay, A. Capon, P. Berry, C. Broderick, R. de Dear, G. Havenith, Y. Honda, R. S. Kovats, W. Ma, and A. Malik, "Reducing the health effects of hot weather and heat extremes: from personal cooling strategies to green cities," *The Lancet*, vol. 398, no. 10301, pp. 709-724, 2021.
- [3] K. L. Ebi, A. Capon, P. Berry, C. Broderick, R. de Dear, G. Havenith, Y. Honda, R. S. Kovats, W. Ma, and A. Malik, "Hot weather and heat extremes: health risks," *The lancet*, vol. 398, no. 10301, pp. 698-708, 2021.
- [4] C. Gabbe, G. Pierce, E. Petermann, and A. Marecek, "Why and how do cities plan for extreme heat?," *Journal of Planning Education and Research*, vol. 44, no. 3, pp. 1316-1330, 2024.
- [5] D. R. Fowler, C. S. Mitchell, A. Brown, T. Pollock, L. A. Bratka, J. Paulson, A. C. Noller, R. Mauskopf, K. Oscanyan, and A. Vaidyanathan, "Heat-related deaths after an extreme heat event—four states, 2012, and United States, 1999–2009," *Morbidity and Mortality Weekly Report*, vol. 62, no. 22, pp. 433, 2013.
- [6] L. Coates, K. Haynes, J. O'brien, J. McAneney, and F. D. De Oliveira, "Exploring 167 years of vulnerability: An examination of extreme heat events in Australia 1844–2010," *Environmental Science & Policy*, vol. 42, pp. 33-44, 2014.
- [7] M. Wehner, D. Stone, H. Krishnan, K. AchutaRao, and F. Castillo, "16. The deadly combination of heat and humidity in India and Pakistan in summer 2015," *Bulletin of the American Meteorological Society*, vol. 97, no. 12, pp. S81-S86, 2016.
- [8] R. Hu, Y. Liu, S. Shin, S. Huang, X. Ren, W. Shu, J. Cheng, G. Tao, W. Xu, and R. Chen, "Emerging materials and strategies for personal thermal management," *Advanced Energy Materials*, vol. 10, no. 17, pp. 1903921, 2020.
- [9] Wu, R., Sui, C., Chen, T.H., Zhou, Z., Li, Q., Yan, G., Han, Y., Liang, J., Hung, P.J., Luo, E., Talapin, D.V., and Hsu, P.C. "Spectrally engineered textile for radiative cooling against urban heat islands". *Science*, vol.384, no. 6701, pp.1203-1212, 2024.
- [10] Zeng, S., Pian, S., Su, M., Wang, Z., Wu, M., Liu, X., Chen, M., Xiang, Y., Wu, J., Zhang, M., Cen, Q., "Hierarchical-morphology metafabric for scalable passive daytime radiative cooling". *Science*, vol. 373, no. 6555, pp.692-696, 2021.
- [11] D. Miao, X. Wang, J. Yu, and B. Ding, "Nanoengineered textiles for outdoor personal cooling and drying," *Advanced Functional Materials*, vol. 32, no. 51, pp. 2209029, 2022.
- [12] B. Liu, R. Zhang, Y. Wu, Y. Wang, T. Yu, X. Li, M. Pu, X. Ma, and X. Luo, "Radiative Cooling and Protective Clothing Through Lamination of Hierarchically Porous Membrane," *Advanced Materials Technologies*, pp. 2301808, 2024.
- [13] E. A. Arens, and H. Zhang, "The skin's role in human thermoregulation and comfort," 2006.
- [14] Y. Peng, W. Li, B. Liu, W. Jin, J. Schaadt, J. Tang, G. Zhou, G. Wang, J. Zhou, and C. Zhang, "Integrated cooling (i-Cool) textile of heat conduction and sweat transportation for personal perspiration management," *Nature communications*, vol. 12, no. 1, pp. 6122, 2021.
- [15] I. Di Domenico, S. M. Hoffmann, and P. K. Collins, "The role of sports clothing in thermoregulation, comfort, and performance during exercise in the heat: a narrative review," *Sports Medicine-Open*, vol. 8, no. 1, pp. 58, 2022.
- [16] C. Ding, Y. Lin, N. Cheng, N. Meng, X. Wang, X. Yin, J. Yu, and B. Ding, "Dual - Cooling Textile Enables Vertical Heat Dissipation and Sweat Evaporation For Thermal and Moisture Regulation," *Advanced Functional Materials*, pp. 2400987, 2024.

- [17] G. Kim, C. Gardner, K. Park, Y. Zhong, and S. Jin, "Human - skin - inspired adaptive smart textiles capable of amplified latent heat transfer for thermal comfort," *Advanced Intelligent Systems*, vol. 2, no. 12, pp. 2000163, 2020.
- [18] Y. Zhong, F. Zhang, M. Wang, C. J. Gardner, G. Kim, Y. Liu, J. Leng, S. Jin, and R. Chen, "Reversible humidity sensitive clothing for personal thermoregulation," *Scientific reports*, vol. 7, no. 1, pp. 44208, 2017.
- [19] X. Li, B. Ma, J. Dai, C. Sui, D. Pande, D. R. Smith, L. C. Brinson, and P.-C. Hsu, "Metalized polyamide heterostructure as a moisture-responsive actuator for multimodal adaptive personal heat management," *Science Advances*, vol. 7, no. 51, pp. eabj7906, 2021.
- [20] J. Zeng, X. Zhang, K. M. Chung, T. Feng, H. Zhang, R. S. Prasher, and R. Chen, "Moisture thermal battery with autonomous water harvesting for passive electronics cooling," *Cell Reports Physical Science*, vol. 4, no. 2, 2023.
- [21] S. Pu, J. Fu, Y. Liao, L. Ge, Y. Zhou, S. Zhang, S. Zhao, X. Liu, X. Hu, K. Liu, and J. Chen, "Promoting energy efficiency via a self - adaptive evaporative cooling hydrogel," *Advanced Materials*, vol. 32, no. 17, pp. 1907307, 2020.
- [22] J. Fei, D. Han, X. Zhang, K. Li, N. Lavielle, K. Zhou, X. Wang, J. Y. Tan, J. Zhong, and M. P. Wan, "Ultrahigh passive cooling power in hydrogel with rationally designed optofluidic properties," *Nano letters*, vol. 24, no. 2, pp. 623-631, 2023.
- [23] X. Hu, P. Hu, L. Liu, L. Zhao, S. Dou, W. Lv, Y. Long, J. Wang, and Q. Li, "Lightweight and hierarchically porous hydrogels for wearable passive cooling under extreme heat stress," *Matter*, 2024.
- [24] Y. Li, C. Ni, R. Cao, Y. Jiang, L. Xia, H. Ren, Y. Chen, T. Xie, and Q. Zhao, "Sprayable porous hydrogel coating for efficient and sustainable evaporative cooling," *Matter*, 2024.
- [25] J. Tollefson, "IPCC climate report: Earth is warmer than it's been in 125,000 years," *Nature*, vol. 596, no. 7871, pp. 171-172, 2021.
- [26] M. Karzani, Y. Ghavidel, and M. Farajzadeh, "Temporal changes in lethal temperatures above 50 C in the northern hemisphere," *Pure and Applied Geophysics*, vol. 179, no. 9, pp. 3377-3390, 2022.
- [27] C. Tuholske, K. Caylor, C. Funk, A. Verdin, S. Sweeney, K. Grace, P. Peterson, and T. Evans, "Global urban population exposure to extreme heat," *Proceedings of the National Academy of Sciences*, vol. 118, no. 41, pp. e2024792118, 2021.
- [28] W. Y. Chen, X. L. Shi, J. Zou, and Z. G. Chen, "Thermoelectric coolers: progress, challenges, and opportunities," *Small Methods*, vol. 6, no. 2, pp. 2101235, 2022.
- [29] T. Cao, X.-L. Shi, and Z.-G. Chen, "Advances in the design and assembly of flexible thermoelectric device," *Progress in Materials Science*, vol. 131, pp. 101003, 2023.
- [30] L. Li, W. D. Liu, Q. Liu, and Z. G. Chen, "Multifunctional wearable thermoelectrics for personal thermal management," *Advanced Functional Materials*, vol. 32, no. 22, pp. 2200548, 2022.
- [31] S. Ren, M. Han, and J. Fang, "Personal cooling garments: a review," *Polymers*, vol. 14, no. 24, pp. 5522, 2022.
- [32] D. Ji, P. Liu, P. Im, S. Shin, and J. Kim, "Thermal Interface Hydrogel Composites Mechanically Compliant with Curvy Skins and Rigid Electronic Modules," *Advanced Functional Materials*, pp. 2402144, 2024.
- [33] Y. Zhang, J. Gao, S. Zhu, J. Li, H. Lai, Y. Peng, and L. Miao, "Wearable thermoelectric cooler based on a two-layer hydrogel/nickel foam heatsink with two-axis flexibility," *ACS Applied Materials & Interfaces*, vol. 14, no. 13, pp. 15317-15323, 2022.

- [34] J. Choi, C. Dun, C. Forsythe, M. P. Gordon, and J. J. Urban, "Lightweight wearable thermoelectric cooler with rationally designed flexible heatsink consisting of phase-change material/graphite/silicone elastomer," *Journal of Materials Chemistry A*, vol. 9, no. 28, pp. 15696-15703, 2021.
- [35] R. A. Kishore, A. Nozariasbmarz, B. Poudel, M. Sanghadasa, and S. Priya, "Ultra-high performance wearable thermoelectric coolers with less materials," *Nature communications*, vol. 10, no. 1, pp. 1765, 2019.
- [36] Y. Xu, Z. Li, J. Wang, M. Zhang, M. Jia, and Q. Wang, "Man-portable cooling garment with cold liquid circulation based on thermoelectric refrigeration," *Applied Thermal Engineering*, vol. 200, pp. 117730, 2022.
- [37] L. Li, W. D. Liu, W. Sun, D. Z. Wang, L. C. Yin, M. Li, X. L. Shi, Q. Liu, and Z. G. Chen, "Performance optimization of a thermoelectric - water hybrid cooling garment," *Advanced Materials Technologies*, pp. 2301069, 2023.
- [38] S. Hong, Y. Gu, J. K. Seo, J. Wang, P. Liu, Y. S. Meng, S. Xu, and R. Chen, "Wearable thermoelectrics for personalized thermoregulation," *Science advances*, vol. 5, no. 5, pp. eaaw0536, 2019.
- [39] R. Kumar, R. Aggarwal, J. Sharma, and S. Pathania, "Predicting energy requirement for cooling the building using artificial neural network," *Journal of Technology Innovations in Renewable Energy*, vol. 1, no. 2, pp. 113, 2012.
- [40] T. Feng, J. Wang, E. Sun, A. Di Buono, and R. Chen, "Flexible Thermoelectric Active Cooling Garment to Combat Extreme Heat," <https://ui.adsabs.harvard.edu/abs/2024arXiv241108349F>, [November 01, 2024].

Supporting Information

Thermoelectrically Elevated Hydrogel Evaporation for Personal Cooling under Extreme Heat Stress

Yu Pei, Tianshi Feng, Robert Chambers, Shengqiang Cai, Renkun Chen**

Yu Pei, Tianshi Feng, Robert Chambers, Shengqiang Cai, Renkun Chen

Department of Mechanical and Aerospace Engineering, University of California San Diego,
9500 Gilman Drive, La Jolla, CA 92093, USA

Shengqiang Cai, Renkun Chen

Program in Materials Science and Engineering, University of California San Diego, 9500 Gilman
Drive, La Jolla, CA 92093, USA

E-mail: shqcai@ucsd.edu; rkchen@ucsd.edu

Supporting Note 1:

Evaporation rate calculation

The amount of evaporated water g_s [$\text{kg s}^{-1} \text{m}^{-2}$] can be described by the equation:

$$g_s = (25 + 19v) * (X_s - X_{sair}) * 3600 \quad (1)$$

where v is the air velocity above the water, which is around 0.1 m s^{-1} in our test environment, X_s is the maximum humidity ratio of saturated air, X_{sair} is the humidity ratio for air.

Based on the ideal gas law the humidity ratio can be expressed as:

$$X = 0.62198 \frac{P_w}{P_a - P_w} \quad (2)$$

where P_w is partial pressure of water vapor in moist air, P_a is the atmospheric pressure of the moist air.

The maximum amount of water vapor in the air is achieved when P_w reaches the saturation pressure $P_{w,s}$ of water vapor at water surface temperature. The maximum humidity ratio of saturated air X_s can be calculated by:

$$X_s = 0.62198 \frac{P_{w,s}}{P_a - P_{w,s}} \quad (3)$$

Saturated water maximum vapor pressure $P_{w,s}$ is a function of temperature only, which can be represented by an empirical formula:

$$P_{w,s} = e^{A + \frac{B}{T} + C \ln T + DT} \quad (4)$$

where T is the temperature in Kelvin,

A = 77.34,

B = -7235,

C = -8.2,

D = 0.005711.

Similarly, the humidity ratio for air X_{sair} is:

$$X_{sair} = 0.62198 * \frac{RH * P_{w,s,air}}{P_a - RH * P_{w,s,air}} \quad (5)$$

where RH is the relative humidity, $P_{w,s,air}$ is the maximum saturation pressure of the water vapor at ambient air temperature.

The mass loss ratio $\frac{m_0 - m}{m_0}$ can be calculated by

$$\frac{m_0 - m}{m_0} = \frac{g_s \cdot t \cdot 60 \cdot A}{m_0} \quad (6)$$

where t [min] is the time, and A [m²] is the surface area of hydrogel.

The heat flux q [W m⁻²] corresponding to each evaporation rate can be expressed as:

$$q = g_s \cdot L_v \quad (7)$$

where L_v is the latent heat of water, $L_v = 2.42 \cdot 10^6$ [J kg⁻¹] at 40°C.

Supporting Note 2:

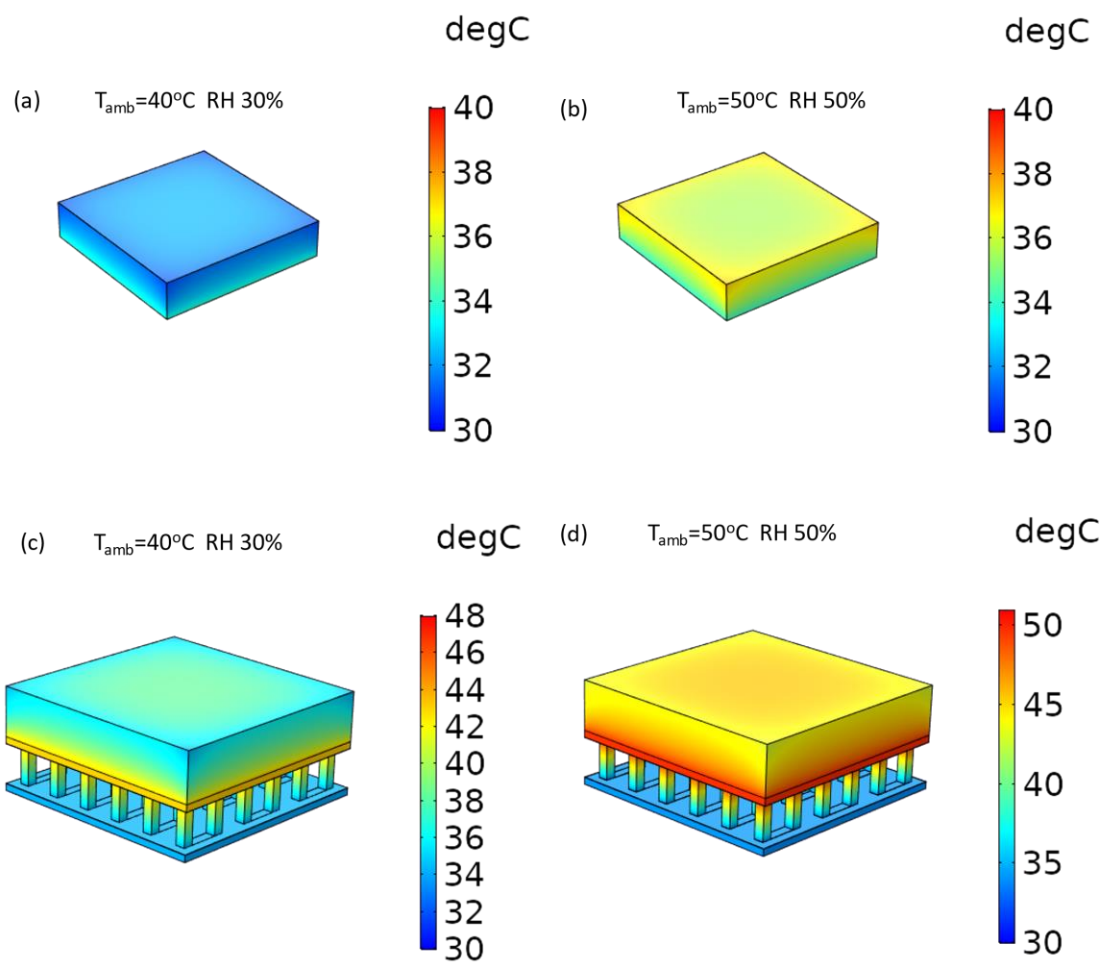


Figure S1. COMSOL simulation result of temperature distribution in hydrogel. Temperature distribution for hydrogel at (a) 40 °C ambient temperature and 30% RH; (b) 50 °C ambient temperature and 50% RH. Temperature distribution for TED-hydrogel device at (c) 40 °C ambient temperature and 30% RH; (d) 50 °C ambient temperature and 50% RH.

Supporting Note 3:

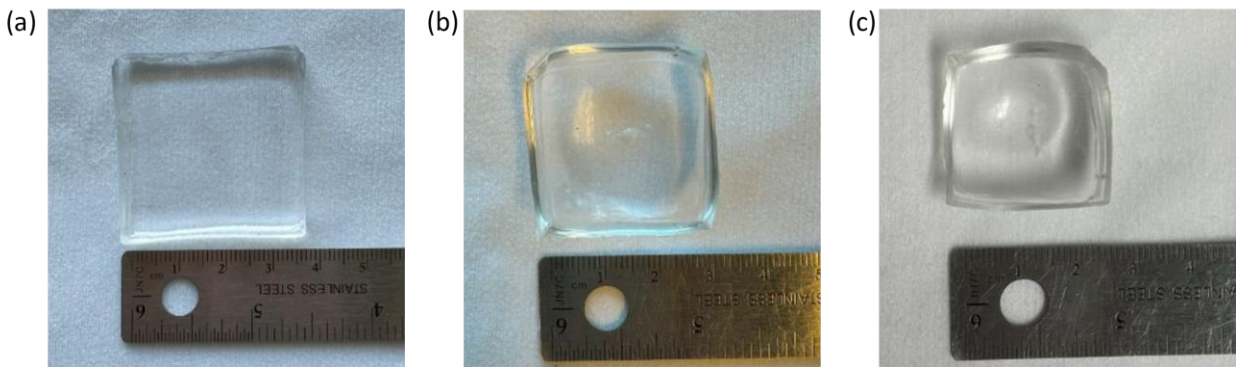


Figure S2. Changes in 5mm thick hydrogel size over test time. (a) Before test (side length ~3.7cm). (b) After 2 hr test (side length ~3cm). (c) After 4 hr test (side length ~2.5cm). Test environment: ambient temperature 50 °C, humidity 30%-35%.

Supporting Note 4:

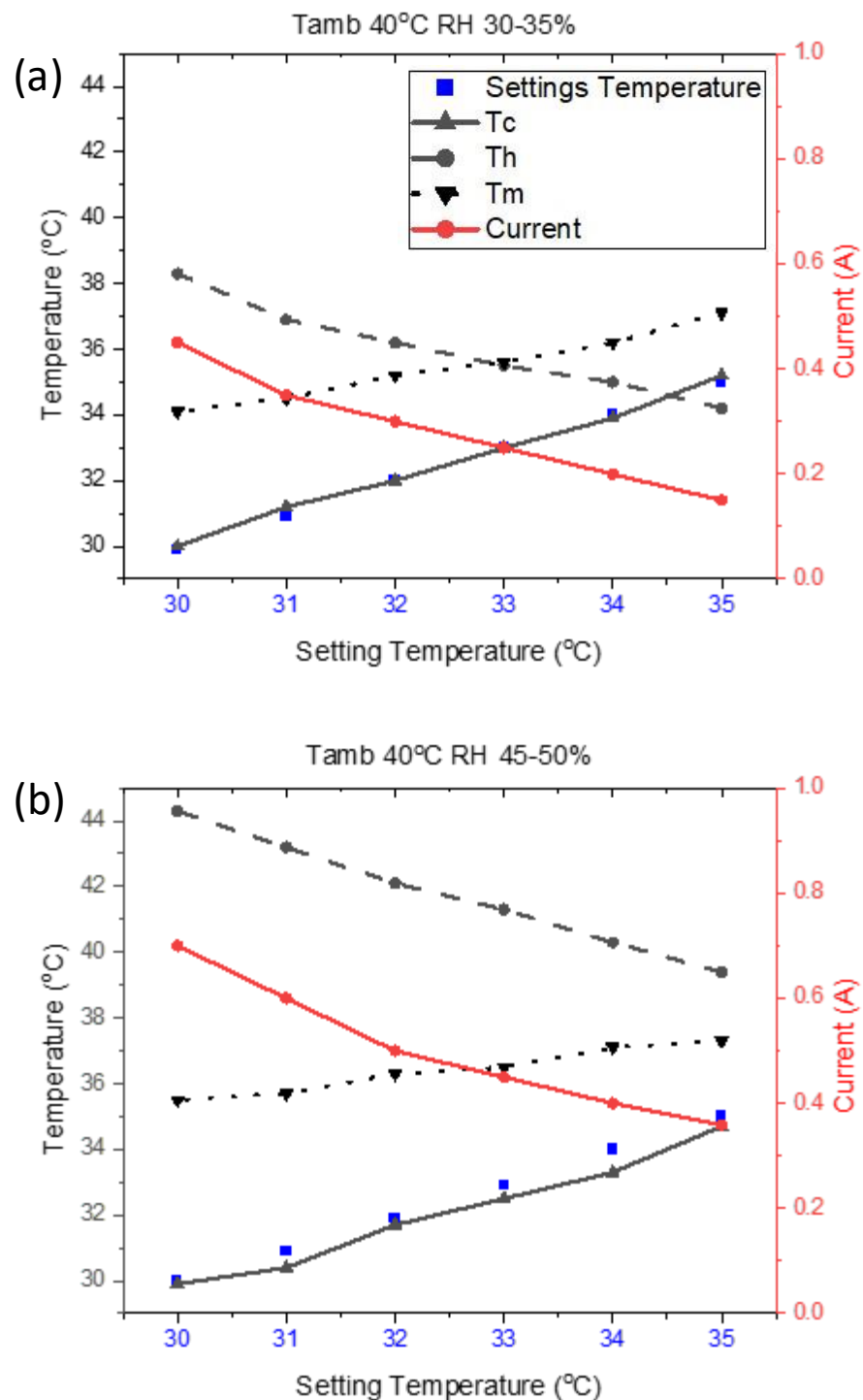


Figure S3. TED-hydrogel garment temperature response under different setting temperature. Ambient temperature at 4 0°C and relative humidity is (a) 30–35% and (b) 45–50%. Hydrogel thickness is 5mm. Heat flux is 100 Wm⁻².